Available online at www.sciencedirect.com
SCIENCE DIRECT
NeuroToxicology 27 (2006) 229–236
NeuroToxicology

Acute manganese administration alters dopamine transporter levels in the non-human primate striatum

Ming-Kai Chen [a], Jae-Sung Lee [b], Jennifer L. McGlothan [a], Eri Furukawa [a], Robert J. Adams [c], Mohab Alexander [b], Dean F. Wong [b], Tomás R. Guilarte [a,*]

[a] Department of Environmental Health Sciences, Johns Hopkins Bloomberg School of Public Health, Baltimore, MD, USA
[b] Department of Radiology, Johns Hopkins School of Medicine, Baltimore, MD, USA
[c] Department of Comparative Medicine, Johns Hopkins School of Medicine, Baltimore, MD, USA

Received 1 August 2005; accepted 19 October 2005
Available online 2 December 2005

Abstract

We used positron emission tomography (PET) to measure non-invasively the effect of acute systemic administration to manganese sulfate ($MnSO_4$) on dopamine transporter (DAT) levels in the living non-human primate brain. Baboons received [^{11}C]-WIN 35,428 PET scans to measure DAT levels before and after acute $MnSO_4$ administration. In one animal, we observed a 46% increase in DAT binding potential (BP), a measure of DAT binding site availability, 1 week after Mn administration. DAT levels returned to baseline values at 4 months and remained constant at 10 months after treatment. A subsequent single $MnSO_4$ injection to the same animal also resulted in a 57% increase in DAT-BP, 2 days after administration. In a second animal, a 76% increase in DAT-BP relative to baseline was observed at 3 days after Mn injection. In this animal, the DAT-BP returned to baseline levels after 1 month. Using in vitro receptor binding assays, we found that Mn inhibits [^{3}H]-WIN 35,428 binding to rat striatal DAT with an inhibitory constant (K_i) of 2.0 ± 0.3 mM ($n = 4$). Saturation isotherms and Scatchard analysis of [^{3}H]-WIN 35,428 binding to rat striatal DAT showed a significant decrease (30%, $p < 0.001$) in the maximal number of binding sites (B_{max}) in the presence of 2 mM $MnSO_4$. No significant effect of Mn was found on binding affinity (K_d). We also found that Mn inhibits [^{3}H]-dopamine uptake with an IC_{50} of 11.4 ± 1.5 mM ($n = 4$). Kinetic studies and Lineweaver–Burk analysis showed a significant decrease (40%, $p < 0.001$) in the maximal velocity of uptake (V_{max}) with 5 mM $MnSO_4$. No significant effect of Mn was found on Michaelis–Menton constant (K_m). These in vitro findings suggest that the increase in DAT levels in vivo following acute Mn administration may be a compensatory response to its inhibitory action on DAT. These findings provide helpful insights on potential mechanisms of Mn-induced neurotoxicity and indicate that the DAT in the striatum is a target for Mn in the brain.

Keywords: Manganism; Dopamine transporter; Manganese sulfate; Positron emission tomography; Non-human primate; Striatum; Parkinson's disease

1. Introduction

Manganese (Mn) is an essential trace element for human nutrition but also a toxicant when humans are exposed to high concentrations. Occupational exposures to excess levels of Mn are known to cause a Parkinsonian-like syndrome in humans (Pal et al., 1999). The neurological manifestation of this Mn-induced syndrome include bradykinesia and rigidity which are similar to idiopathic Parkinson's disease (IPD) (Pal et al., 1999). However, there are clinical distinctions between IPD and Mn-induced parkinsonism. In Mn-induced parkinsonism there is action tremor and absence of resting tremor, more dystonia, and severe gait disturbance ''cock-walk'' with difficulty in backward walking and no response to levodopa therapy (Kim et al., 2002; Pal et al., 1999). The globus pallidus and striatum are basal ganglia structures that exhibit high levels of Mn accumulation visualized by T1-weighted magnetic resonance imaging (MRI) following Mn exposure (Eriksson et al., 1992b; Nelson et al., 1993; Newland et al., 1989; Newland and Weiss, 1992). The major pathological findings in manganism include a prominent decrease of myelinated fibers, gliosis and the degeneration of neurons in the globus pallidus and caudate/putamen (Olanow et al., 1996; Yamada et al., 1986). There is also an apparent sparing of the substantia nigra pars compacta

* Corresponding author. Present address: Department of Environmental Health Sciences, The Johns Hopkins University, Bloomberg School of Public Health, 615 North Wolfe Street, Room E6622, Baltimore, MD 21205, USA. Tel.: +1 410 955 2485; fax: +1 410 502 2470.
E-mail address: tguilart@jhsph.edu (T.R. Guilarte).

0161-813X/$ – see front matter
doi:10.1016/j.neuro.2005.10.008

(Olanow et al., 1996), the brain region that is affected in IPD. Although early reports suggest that the clinical picture and pathophysiology of manganism are distinct from PD, there are case reports of PD patients with a history of Mn exposure (Kim et al., 2002). Further, welders exposed to high levels of Mn have recently been described to have a higher prevalence of PD at an early age (Racette et al., 2001, 2005). These reports suggest that Mn exposure is an important risk factor for IPD.

The organomanganese compound methylcyclopentadienyl manganese tricarbonyl (MMT) has been approved in the United States, Canada and other parts of the world as an alternative antiknock additive in gasoline. Upon combustion in an automobile engine, MMT yields a mixture of sulfate, phosphate and dioxide complexes of Mn with the sulfate and phosphate forms being the major emission products (Lynam et al., 1999). Thus, it is likely that extensive use of MMT-containing gasoline may increase Mn exposure levels to the general population. Therefore, a better understanding of the pathophysiology of Mn-induced neurotoxicity and the development of appropriate biomarkers for in vivo detection is needed.

Positron emission tomography (PET) is a non-invasive imaging technique that has been widely used to visualize the biochemistry of the living brain. In this study, we used PET with the dopamine transporter (DAT) selective radioligand [^{11}C]-WIN 35,428 (Dannals et al., 1993; Wong et al., 1993) to measure the effect of acute exposure to manganese sulfate ($MnSO_4$) on DAT levels in the corpus striatum as an index of dopaminergic neuron toxicity. Our results show that acute Mn administration produces a transient increase in [^{11}C]-WIN 35,428 binding to DAT in the striatum in vivo. To the best of our knowledge, this is the first report of an increase in striatal DAT binding potential (BP), a measure of binding site availability, from acute Mn administration using in vivo PET imaging. To investigate the molecular mechanisms of this acute effect of Mn-induced dopaminergic dysfunction, we used in vitro assays to measure the effects of Mn on the binding of [^{3}H]-WIN 35,428 to DAT from rat striatal membranes and the uptake kinetics of [^{3}H]-dopamine by DAT from rat striatal synaptosomes. The results indicate that Mn inhibits both the binding of [^{3}H]-WIN 35,428 to DAT in rat striatal membranes and the uptake of [^{3}H]-DA by DAT into rat striatal synaptosomes. These in vitro findings suggest that the increase in DAT levels in vivo following acute Mn administration may be a compensatory response to its inhibitory action on the transporter. We suggest that DAT in striatal dopaminergic terminals is a target for Mn in the brain.

2. Material and method

2.1. Animals and manganese treatment

Two adult male baboons (*Papio anubis*) with unremarkable histories and weighing 25–30 kg were used in this study. Baboons were singled housed in a colony room maintained at 22 ± 1 °C, with free access to food (2050 Protein Primate Diet; Harland Teklad, Madison, WI) and water. Food was supplemented by fruits and other treats. Animals were sedated (8–15 mg/kg ketamine, IM) prior to Mn treatment. Manganese sulfate (10–50 mg/kg in sterile saline) was administered by either subcutaneous or intravenous injection using an infusion pump over a period of 10 min. The injection volume was less than 5 ml for subcutaneous and 10 ml for intravenous. It is important to mention that the subcutaneous administration of $MnSO_4$ causes severe irritation at the site of injection and this route of exposure should be avoided. We initially performed two subcutaneous injection of $MnSO_4$ in one baboon referencing previous studies (Eriksson et al., 1987, 1992a) and after experiencing this complication on two occasions, the route of administration was changed to intravenous (i.v.) injection with no complication. All animal protocols (primate and rat) were approved by the Animal Care and Use Committee of the Johns Hopkins Medical Institutions.

2.2. PET imaging acquisition and analysis

Baseline and a series of post Mn treatment PET studies were performed. On the day of the PET study, two intravenous catheters and an arterial catheter were placed for infusion of anesthesia, injection of radiotracer, and arterial blood sampling, respectively. Animals were initially anesthetized intramuscularly with 8–10 mg/kg Saffan®, a formulation that contains 9 mg/ml alfaxalone and 3 mg/ml alfadolone acetate (Arnolds Veterinary Products, Shropshire, UK). Animals were maintained throughout the study by a continuous intravenous infusion drip of 6–9 mg kg^{-1} h^{-1} Saffan®. To ensure reproducibility of positioning during the multiple PET studies, a custom-made thermoplastic facemask (Tru Scan Imaging, Annapolis, MD) was fitted to the baboon's head, which was then attached to the head holder during the PET scans. The laser light in the PET scanner matched markings on the facemask to ensure the exact head position in each study. After baboons were positioned in the PET scanner, a transmission scan was obtained with twin 370 MBq (10 mCi) ^{68}Ge pin sources for 10 min and used for attenuation correction of the subsequent emission PET scans. PET scanning started immediately after intravenous injection of 20 mCi of high specific activity [^{11}C]-WIN 35,428 that was synthesized as described previously (Dannals et al., 1993). The average specific activity of the final product calculated at end of synthesis was >2000 mCi/μmol with a radiochemical purity >95%. A GE Advance PET camera (General Electric) with an axial resolution (full width at half maximum) of 5.8 mm and an in-plane resolution of 5.4 mm was used for image acquisition. This scanner acquires 35 simultaneous slices of 4.25-mm thickness, enclosing a total longitudinal field of view of 15 cm. Thirty serial dynamic PET images were acquired during the 90 min after injection of radioligand using the following image sequence: 4 × 15 s frames, 4 × 30 s frames, 3 × 1 min frames, 2 × 2 min frames, 5 × 4 min frames, and 12 × 5 min frames. In all cases, over 32 arterial samples/PET study (for radioactivity) were obtained during the 90 min acquisition time. Arterial samples were also obtained at 5, 10, 15, 30, 60, and 90 min after the injection of the radiotracer for analysis by means of high performance liquid chromatography (HPLC) for the correction of the metabolism of [^{11}C]-WIN 35,428. PET scans were recon-

structed using ramp-filtered back-projection in a 128 × 128 matrix, with a transaxial pixel size of 2 mm × 2 mm. Images were corrected for attenuation and decay. Regions of interest were placed manually over the striatum and the cerebellum, and time–activity curves (TAC) were generated (Fig. 1A and B).

One-tissue and two-tissue compartmental models were used to fit the time–activity curves for cerebellum and striatum, respectively, using metabolite-corrected arterial blood activity as the input function (Fig. 2). Binding potential (BP) (i.e., B_{max}/K_d), which represents the k_3/k_4 ratio in striatum was determined in each study using a previously described method (Wong et al., 1993).

2.3. Effect of $MnSO_4$ on [^{3}H]-WIN 35,428 binding to DAT from rat striatal membranes

Adult male Long Evans rats (250–350 g; Charles River, Wilmington, MA, USA) were housed in plastic cages with bedding at 22 ± 2 °C under a 12-h light:12-h dark cycle. Animals were euthanized by decapitation and striatal tissue was dissected and homogenized in 45 volumes of 0.32 M sucrose at 4 °C and centrifuged at 1000 × g for 10 min. The supernatant was centrifuged at 17,000 × g for 20 min, the resulting pellet (P_2) was resuspended in 50 mM Tris–HCl buffer (pH 7.4) with 100 mM NaCl and used for the radioligand-binding assay methods as described by Coffey and Reith (1994) with modification. For inhibition studies, 13 different concentrations of manganese sulfate ($MnSO_4$) (from 1 nM to 10 mM) were added to 2.8 nM [^{3}H]-WIN 35,428 (Perkin-Elmer LAS Inc. Shelton, CT, USA). For Scatchard analysis, total binding of [^{3}H]-WIN 35,428 was determined with concentrations ranging from 0.25 to 50 nM with or without 2 mM $MnSO_4$. Non-specific binding was assessed for each [^{3}H]-WIN 35,428 concentration in the presence of 100 μM of the DAT inhibitor, GBR 12909 (Sigma, St. Louis, MO). Binding reaction mixtures were incubated for 120 min at 4 °C in a total volume of 500 μl. The reaction was terminated by vacuum filtration through GF/B filters, followed by three washes with 5 ml of ice-cold buffer. Radioactivity trapped in the filters was measured by liquid scintillation spectrometry. Protein concentrations of tissue homogenates were determined by the Bradford protein assay. Binding parameters were estimated using the LIGAND in KELL Version 6 program for Windows (Biosoft, Cambridge, UK).

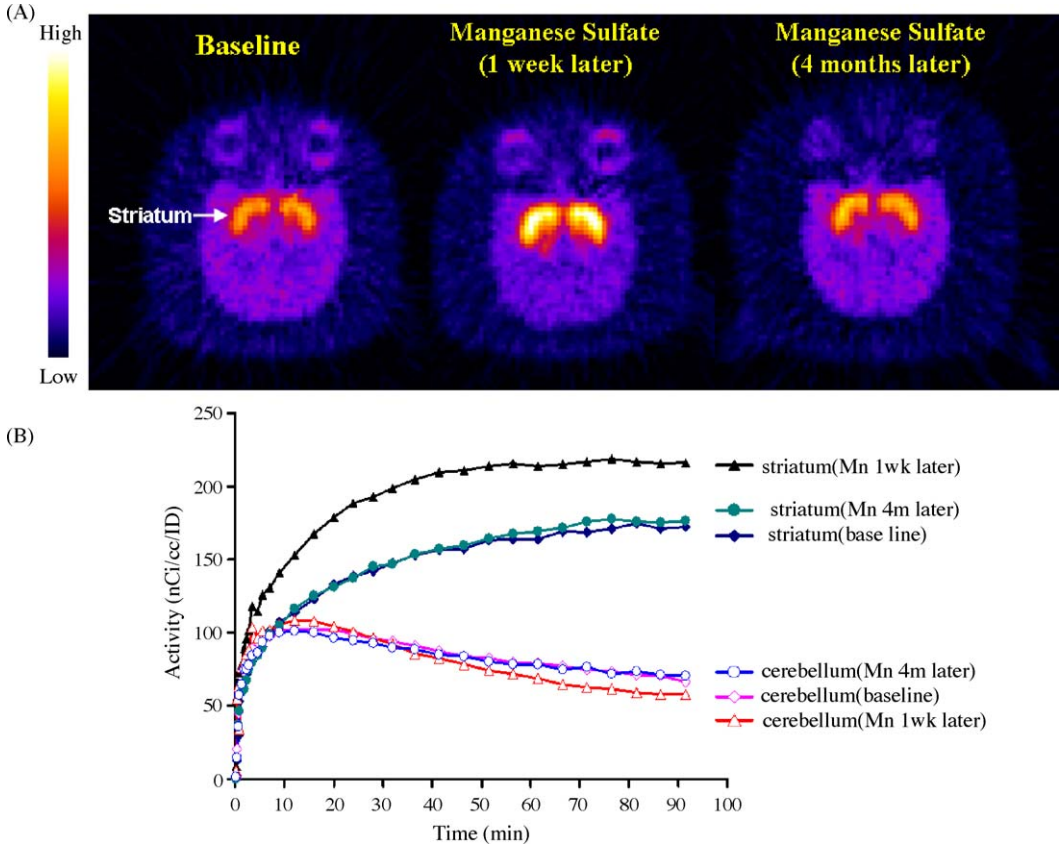

Fig. 1. (A) Representative transaxial images of the distribution of [^{11}C]-WIN 35,428 radioactivity in the baboon brain at the level of the striatum (75–90 min after tracer injection). The bright yellow areas represent a high level of [^{11}C]-WIN 35,428 binding to dopamine transporters (DAT) in the striatum. The activity of [^{11}C]-WIN 35,428 in the striatum increased 1 week after manganese treatment and return to baseline levels after 4 months remaining constant at 10 months (data not shown). The color scale on the left represent the levels of [^{11}C]-WIN 35,428 binding to DAT. (B) Brain tissue time–activity curves acquired from PET imaging analysis of the striatum and cerebellum in the same animal before and after acute manganese administration. There is a dramatic increase of TAC in striatum after 1 week of manganese treatment (50 mg/kg × 2, s.c.) compared to baseline level, and the TAC level recovers to baseline after 4 month. There is no change in the TAC in the cerebellum (regions of non-specific binding) after manganese treatment. Thus, the effect of Mn was selective to DAT in the striatum.

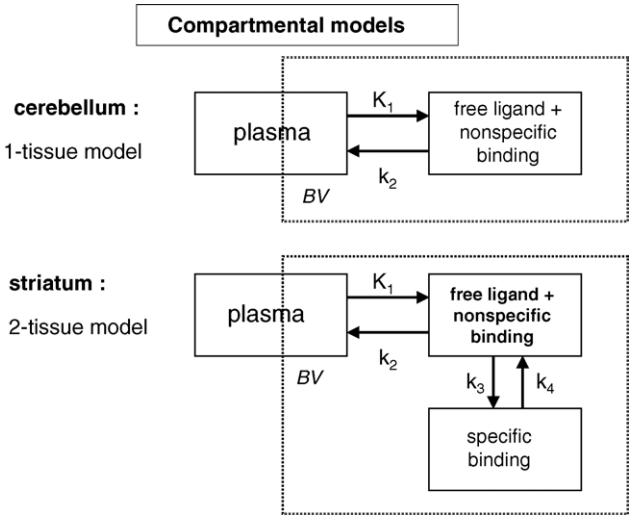

Fig. 2. Kinetic compartmental models to obtain binding potential (BP). We use one-tissue and two-tissue compartmental models to fit the TAC of cerebellum and striatum, respectively, using metabolite-corrected arterial blood activity as the input function. We assume that there is no specific binding of [^{11}C]-WIN 35,428 in the cerebellum (since it contains little or no dopamine transporters), and the K_1/k_2 values are identical in both cerebellum and striatum. In this approach, K_1/k_2 obtained in the cerebellum was used to constrain K_1/k_2 in the striatum, thereby reducing the number of parameters. Binding potential (BP) (i.e., B_{max}/K_d), which represents the k_3/k_4 ratio in striatum was determined in each study. Parameter K_1 was used to describe radioligand uptake in brain and k_2 was used to describe radioligand washout from the brain. For the two-tissue compartment model, k_3 and k_4 were included to describe binding and release of the radioligand at the site of the DAT. The blood activity present in the PET scanner field of view is described by parameter BV.

2.4. Effect of $MnSO_4$ on [^{3}H]-dopamine uptake in rat striatal synaptosomes

Striatal tissue was dissected and homogenized in 20 volumes of 0.32 M sucrose, 50 mM Tris–HEPES (pH 7.4) at 4 °C and centrifuged at 900 × *g* for 10 min. The supernatant was centrifuged at 17,000 × *g* for 20 min. The pellet was resuspended in ice-cold incubation buffer and mixed by vortexing. The incubation buffer consisted of 10 mM Tris–HEPES, pH 7.4 (145 mM NaCl, 5 mM KCl, 1 mM $MgCl_2$, 1 mM $CaCl_2$, 10 mM glucose, 0.25 mM ascorbate and 15 μM pargyline (Barlow et al., 2003). For inhibition studies, 11 different concentrations of $MnSO_4$ from 1 μM to 50 mM were used. [^{3}H]-DA (Perkin-Elmer LAS Inc.) was used at a concentration of 10 nM. For kinetic analysis, 11 different concentrations (from 50 to 3000 nM) of DA were used as a mixture of 50 nM [^{3}H]-DA with various concentrations of unlabelled DA. The synaptosomal preparation was pre-incubated for 15 min at 37 °C with or without 5 mM $MnSO_4$. Uptake reactions were triggered by adding [^{3}H]-DA and incubated for 3 min at 37 °C in a total volume of 500 μl. Non-specific uptake was determined by incubation at 4 °C or adding 100 μM GBR 12909 at 37 °C, both produced similar results. The reaction was terminated by adding 1 ml of cold buffer and vacuum filtration through GF/B filters, followed by three washes with 5 ml of ice-cold buffer. Radioactivity trapped in the filters was measured by liquid scintillation spectrometry. The IC_{50} value was obtained using LIGAND program. The K_m and V_{max} were determined by Lineweaver–Burk model with linear regression using SigmaPlot 8.0 (SPSS Inc., Chicago, IL, USA).

3. Results

3.1. Acute administration of manganese results in a transient increase in [^{11}C]-WIN 35,428 binding to DAT in the striatum

Using PET imaging, we visualized striatal DAT levels in the living non-human primate brain and prospectively assessed the

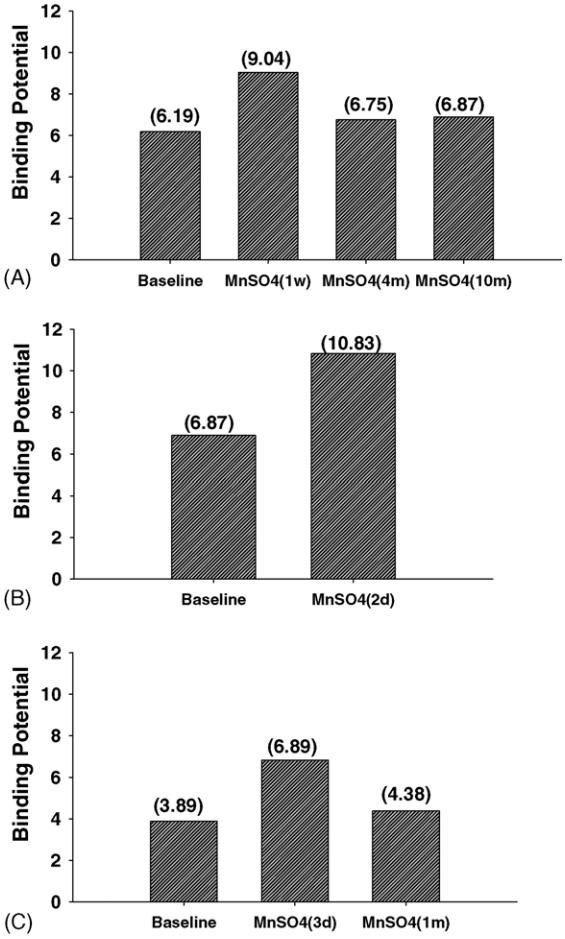

Fig. 3. (A) Effect of acute $MnSO_4$ administration on DAT binding potential (BP) in striatum (animal #1, 50 mg/kg × 2, s.c.). A 46% increase from a baseline of 6.19 to 9.04 after 1 week of $MnSO_4$ treatment was measured. DAT levels returned to baseline values at 4 months (BP = 6.75) and remained constant at 10 months (BP = 6.87). (B) Effect of acute $MnSO_4$ administration on DAT binding potential in striatum (animal #1, 10 mg/kg, i.v.). The increased DAT binding potential (57%) in striatum (BP = 10.83) can be repeated in the same animal when injected with a single dose of $MnSO_4$ (10 mg/kg) followed by a PET study 2 days later. (C) Effect of acute $MnSO_4$ administration on DAT binding potential in striatum (animal #2, 20 mg/kg, i.v.). A similar result of increased DAT binding potential in striatum was noted in a different animal. A 76% increase in DAT BP was measured from a baseline value of 3.89 to 6.89 at 3 days after $MnSO_4$ injection (20 mg/kg, i.v.). In this animal, the BP returned to baseline (BP = 4.38) at 1 month after $MnSO_4$ administration.

effect of acute $MnSO_4$ administration in the same animal (Fig. 1A). Fig. 1B shows time–activity curves in the striatum and cerebellum, a measurement of [^{11}C]-WIN 35,428 binding to DAT, from the PET imaging during the 90 min scan at different stages of $MnSO_4$ treatment. Using kinetic compartmental modeling (Fig. 2), [^{11}C]-WIN 35,428 binding parameters to DAT were estimated. In one animal, we measured a 46% increase in DAT binding potential (BP) from a baseline of 6.19 to 9.04 1 week after two $MnSO_4$ injections (50 mg/kg, s.c., 1 week apart) (Fig. 3A). In this animal, striatal DAT levels returned to baseline values at 4 months (BP = 6.75) (Fig. 3A) and remained constant at 10 months (BP = 6.87) after treatment. A subsequent single $MnSO_4$ injection (10 mg/kg, i.v.) to the same animal after 22 months from the first $MnSO_4$ treatment also resulted in a 57% increase in DAT-BP from 6.87 to 10.83, 2 days after administration (Fig. 3B). In a second animal, a 76% increase in DAT BP was measured from a baseline value of 3.89 to 6.83 at 3 days after $MnSO_4$ injection (20 mg/kg, i.v.) (Fig. 3C). In this animal, the DAT-BP returned to baseline levels (BP = 4.38) after 1 month (Fig. 3C). These findings suggest that acute Mn administration result in a transient increase in [^{11}C]-WIN 35,428 binding to DAT in the non-human primate striatum.

3.2. *In vitro inhibition of [^{3}H]-WIN 35,428 binding to DAT in the rat striatum by $MnSO_4$*

In order to examine potential mechanism(s) by which acute Mn administration transiently increases DAT levels in vivo, we used in vitro receptor binding assays to measure the effect of Mn on [^{3}H]-WIN 35,428 binding to DAT in rat striatal membranes. Fig. 4A shows that Mn inhibits [^{3}H]-WIN 35,428 binding to rat striatal DAT with a inhibitory constant K_i of 2.0 ± 0.3 mM ($n = 4$). There was no difference on DAT inhibition between $MnSO_4$ and $MnCl_2$ in two different experiments (data not shown). In order to determine how Mn inhibits [^{3}H]-WIN 35,428 binding to DAT, we performed [^{3}H]-WIN 35,428 saturation isotherms in the presence or absence of 2 mM $MnSO_4$ (Fig. 4B). By converting the saturation graphs (Fig. 4B) to linear Scatchard plots (Fig. 4C), we estimated the maximal number of available binding sites (B_{max}) and binding affinity represented by the dissociation constant (K_d) (Fig. 4D). There was a significant

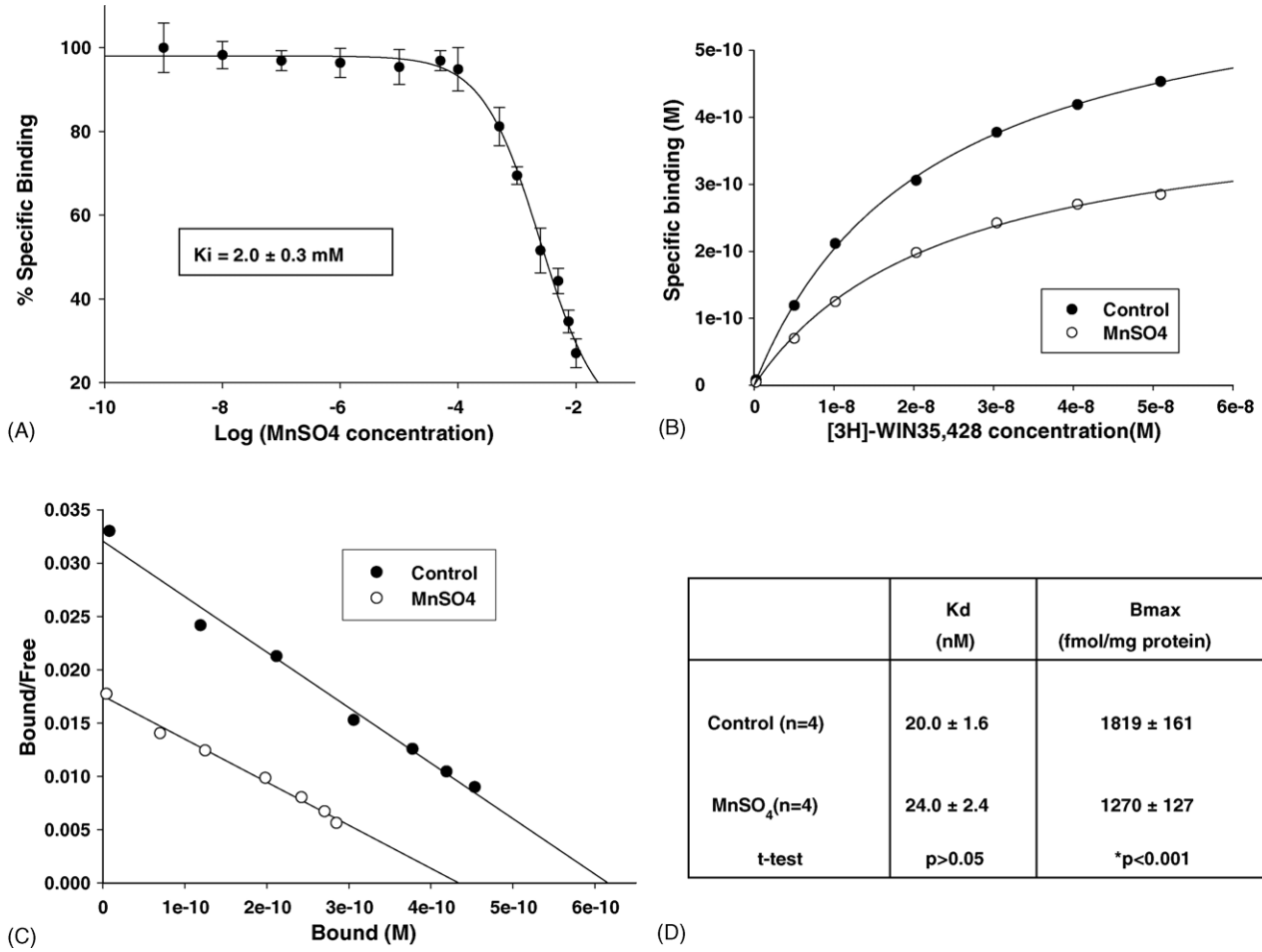

	Kd (nM)	Bmax (fmol/mg protein)
Control (n=4)	20.0 ± 1.6	1819 ± 161
$MnSO_4$(n=4)	24.0 ± 2.4	1270 ± 127
t-test	p>0.05	*p<0.001

(D)

Fig. 4. (A) Effect of $MnSO_4$ on [^{3}H]-WIN 35,428 specific binding to rat striatal DAT. Specific binding values are in fmol/mg protein (B) Representative saturation isotherms of [^{3}H]-WIN 35,428 binding to rat striatal DAT with or without $MnSO_4$ (2 mM). (C) Representative Scatchard plot of [^{3}H]-WIN 35,428 binding to rat striatal DAT with or without $MnSO_4$ (2 mM). (D) Summary of Scatchard analysis ([^{3}H]-WIN 35,428 binding parameters) (mean ± S.E.M.). Each value is the mean ± S.E.M. of four different determinations.

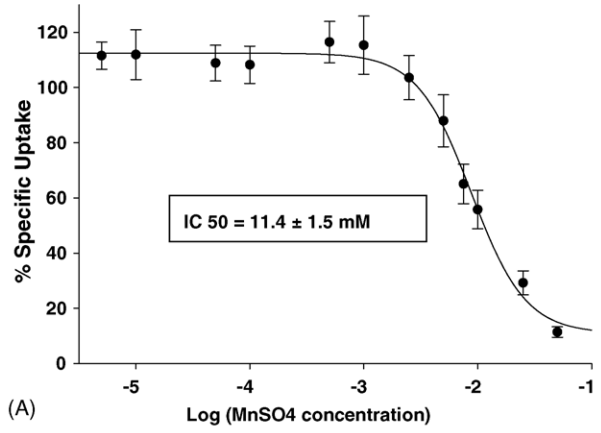

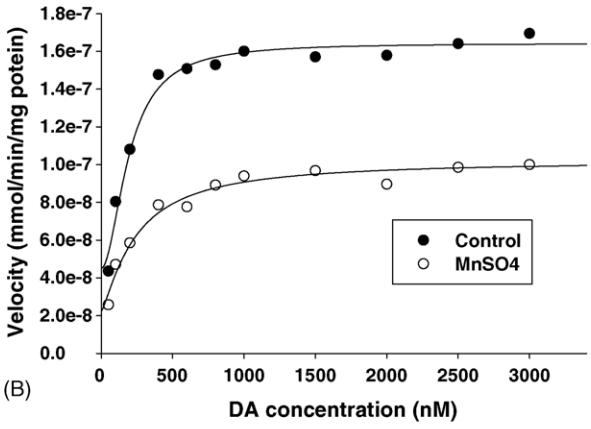

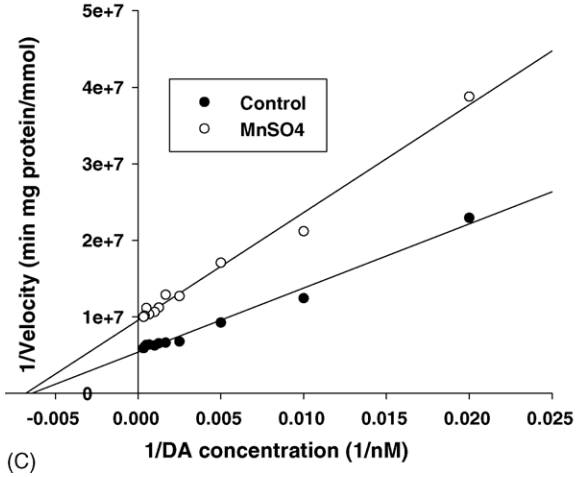

	Km (nM)	Vmax (mmol/min/ mg protein)
Control (n=4)	158.9 ± 29.8	1.86 ± 0.31E-7
$MnSO_4$(n=4)	148.0 ± 64.3	1.05 ± 0.31E-7
t-test	p=0.73	*p=0.003

(D)

Fig. 5. (A) Effect of $MnSO_4$ on percent specific [^{3}H]-DA uptake in rat striatal DAT synaptosome. Specific dopamine uptake values are in mmol/min/mg protein (B) Representative Michaelis–Menten plots of [^{3}H]-DA uptake in rat striatal synaptosomes with or without $MnSO_4$ (5 mM). (C) Representative Lineweaver–Burk plots on DA uptake kinetics in rat striatal synaptosomes with or without $MnSO_4$ (5 mM). (D) Summary of [^{3}H]-DA uptake kinetics (mean ± S.E.M.). Each value is the mean ± S.E.M. of four different determinations.

decrease (30%, $p < 0.001$) in B_{max} in the presence of 2 mM $MnSO_4$ (1270 ± 127 fmol/mg protein, $n = 4$) relative to controls (1819 ± 161 fmol/mg protein, $n = 4$) (Fig. 4D). No significant effect of Mn on K_d was measured (control 20.0 ± 1.6 nM; $MnSO_4$ 24.0 ± 2.4 nM, $p > 0.05$, $n = 4$) (Fig. 4D). These findings suggest that Mn inhibit [^{3}H]-WIN 35,428 binding to DAT in a non-competitive fashion.

3.3. $MnSO_4$ alters the function of the DAT by decreasing the maximal velocity of dopamine uptake (V_{max}) with no change in substrate affinity (K_m)

To further investigate the effect of Mn on DAT function, we performed [^{3}H]-dopamine (DA) uptake assays in rat striatal synaptosomal preparations. High concentrations of Mn inhibited [^{3}H]-DA uptake of rat striatal synaptosomes with an IC_{50} value of 11.4 ± 1.5 mM ($n = 4$) (Fig. 5A). Kinetic analysis of [^{3}H]-DA uptake in the presence or absence of 5 mM $MnSO_4$ resulted in a significant decrease (40%) in V_{max} (control: 1.86 ± 0.31E−7 mmol/min/mg protein; $MnSO_4$: 1.05 ± 0.31E−7 mmol/min/mg protein, $p = 0.003$, $n = 4$). No significant change on K_m (control: 158.9 ± 29.8 nM; $MnSO_4$: 148.0 ± 64.3 nM, $p = 0.73$, $n = 4$)(Fig. 5D) was observed.

4. Discussion

The present study shows that acute administration of Mn results in a transient increase (46–76%) in [^{11}C]-WIN 35,428 binding to DAT in the living non-human primate striatum. These acute effects of Mn on DAT are different from previous reports using chronic Mn treatment and may represent an early event on the effects of Mn on the dopaminergic system. Previous PET studies in Mn-exposed non-human primates show a 60% reduction of [^{11}C]-nomifensine binding to DAT after chronic administration of MnO_2 (12 injections of 0.4 g over 16 months with total accumulation around 1200 mg/kg) (Eriksson et al., 1992b). Single photon emission computed tomography (SPECT) studies in humans exposed to Mn show 6–9 or 57–72% reductions of DAT level using [^{99m}Tc]TRO-DAT-1 or [^{123}I]β-CIT, respectively (Huang et al., 2003; Kim et al., 2002). Other studies also show decreased DAT level (75%) after chronic Mn treatment using [^{3}H]-mazindol quantitative autoradiography in postmortem monkey brain (Eriksson et al., 1992a). In contrast, the present findings demonstrate that acute Mn administration causes a transient increased in DAT levels, an effect that is different from those produced by chronic Mn administration.

There are several possible scenarios that can explain the transient increase in [^{11}C]-WIN 35,428 binding in the non-human primate striatum after Mn administration. First, acute administration of Mn may decrease synaptic dopamine (DA) concentrations. A Mn-induced decrease in synaptic DA concentrations reduces the ability of endogenous DA to compete with [^{11}C]-WIN 35,428 for binding to DAT resulting in an apparent increase in [^{11}C]-WIN 35,428 binding potential. There are reports indicating that chronic Mn administration to non-human primates decreases the level of DA in the caudate and putamen (Eriksson et al., 1987; Neff et al., 1969) and in rat striatum (Ingersoll et al., 1999). However, there is no evidence for the same effect using acute Mn administration.

Secondly, Mn may cause an up-regulation of DAT protein in the pre-synaptic terminal. Increased DAT protein provides a greater number of binding sites for [^{11}C]-WIN 35,428 binding and may represent a dynamic response of DAT to Mn inhibition. The later possibility is more likely to explain the in vivo findings because our in vitro studies indicate that Mn can inhibit the binding of [^{3}H]-WIN 35,428 to DAT (Fig. 4) and the uptake of [^{3}H]-DA in striatal synaptosomes (Fig. 5). Studies with DAT blockers such as cocaine have shown that it can produce a rapid upregulation of DAT both in vivo and in vitro (Gulley and Zahniser, 2003; Mortensen and Amara, 2003). Thus, it is possible that the inhibitory effects of Mn on transporter function measured in the present study may explain the in vivo effects of acute Mn administration as a compensatory upregulation of DAT levels.

An important question raised by the in vivo studies is whether the acute doses of Mn administered to the animal are relevant to environmental or occupational exposures. The lowest dose given to one of the animals was 10 mg $MnSO_4$/kg body weight (3.25 mg/kg of Mn free salt injected). This dose was able to produce an increase in [^{11}C]-WIN 35,428 binding potential of 57% 2 days after injection. This Mn-induced effect on [^{11}C]-WIN 35,428 binding potential was very similar to that produced by higher doses of Mn (Fig. 3). It is possible that the in vivo effect of Mn on DAT levels may be maximal (i.e., we have a ceiling effect) and it may occur at lower levels of exposure than those used in the present study. An equally important question is related to the relatively high levels of Mn, in the mM range, needed to inhibit the binding of [^{3}H]-WIN 35,428 to DAT from rat striatum and the uptake of [^{3}H]-DA from rat striatal synaptosomes (Figs. 4 and 5). In this respect, it is known that rodents are significantly less sensitive to Mn neurotoxicity than non-human primates and humans (Aschner et al., 2005; Boyes and Miller, 1998). Thus, it is possible that the inhibitory effect of Mn on [^{3}H]-WIN 35,428 binding to DAT from rat striatum and the uptake of [^{3}H]-DA from rat striatal synaptosomes may occur at lower concentrations if the in vitro studies had been performed with non-human primate striatal tissue.

Lastly, it is important to discuss the potential significance of the in vivo Mn-induced increase in [^{11}C]-WIN 35,428 binding potential in the striatum since it may be reflective of increased DAT levels at the synapse. It has been proposed that DAT, may act as a vulnerability factor for dopaminergic neurons in that it may serve as a gateway for the uptake of potentially toxic DA metabolites or putative environmental toxins that can be transported by DAT (Miller et al., 1999). The best known example is the dopaminergic neurotoxicant MPP+ (Miller et al., 1999). In this respect, a previous study has suggested that the uptake of Mn into DAT-expressing brain structures can be markedly reduced by prior administration of cocaine or reserpine (Ingersoll et al., 1999). On the other hand, the uptake of Mn into the cerebellum, a brain region expressing little or no level of dopaminergic innervation or DAT was not affected. Thus, it appears that Mn uptake into DAT-containing brain structures can be decreased by compounds that block DA uptake (i.e., cocaine) thus compete with Mn for uptake by DAT. These findings suggest that the increase in striatal DAT induced by acute Mn administration in the striatum of non-human primates may represent an early event in Mn neurotoxicity that may predispose the dopaminergic neuron to damage by the increased uptake of dopamine or other toxins. These preliminary findings provide helpful insights on potential mechanisms of Mn-induced neurotoxicity and indicate that the DAT in striatal dopaminergic terminals is a target for Mn in the primate brain.

Acknowledgements

This work was supported by NIEHS ES07062 & ES10975 to TRG, and NIDA K24DA00412 to DFW.

References

Aschner M, Erikson KM, Dorman DC. Manganese dosimetry: species differences and implications for neurotoxicity. Crit Rev Toxicol 2005;35:1–32.

Barlow BK, Thiruchelvam MJ, Bennice L, Cory-Slechta DA, Ballatori N, Richfield EK. Increased synaptosomal dopamine content and brain concentrations of paraquat produced by selective dithiocarbamates. J Neurochem 2003;85:1075–86.

Boyes WK, Miller DB. A review of rodent models of manganese neurotoxicity. Neurotoxicology 1998;19:468 [abstract].

Coffey LL, Reith ME. [^{3}H]WIN 35, 428 binding to the dopamine uptake carrier. I. Effect of tonicity and buffer composition. J Neurosci Methods 1994;51:23–30.

Dannals R, Neumeyer J, Milius R, Ravert H, Wilson A, Wagner JH. Synthesis of a radiotracer for studying dopamine uptake sites in vivo using PET: 2b-carbomethoxy-3b-(4-fluorophenyl)-[N-11C-methyl]tropane ([^{11}C]CFT or [^{11}C]WIN-35,428). J Label Comp Radiopharmacol 1993;33:147–52.

Eriksson H, Lenngren S, Heilbronn E. Effect of long-term administration of manganese on biogenic amine levels in discrete striatal regions of rat brain. Arch Toxicol 1987;59:426–31.

Eriksson H, Gillberg PG, Aquilonius SM, Hedstrom KG, Heilbronn E. Receptor alterations in manganese intoxicated monkeys. Arch Toxicol 1992a;66:359–64.

Eriksson H, Tedroff J, Thuomas KA, Aquilonius SM, Hartvig P, Fasth KJ, et al. Manganese induced brain lesions in *Macaca fascicularis* as revealed by positron emission tomography and magnetic resonance imaging. Arch Toxicol 1992b;66:403–7.

Gulley JM, Zahniser NR. Rapid regulation of dopamine transporter function by substrates, blockers and presynaptic receptor ligands. Eur J Pharmacol 2003;479:139–52.

Huang CC, Weng YH, Lu CS, Chu NS, Yen TC. Dopamine transporter binding in chronic manganese intoxication. J Neurol 2003;250:1335–9.

Ingersoll RT, Montgomery EB Jr, Aposhian HV. Central nervous system toxicity of manganese. II: Cocaine or reserpine inhibit manganese concentration in the rat brain. Neurotoxicology 1999;20:467–76.

Kim Y, Kim JM, Kim JW, Yoo CI, Lee CR, Lee JH, et al. Dopamine transporter density is decreased in Parkinsonian patients with a history of manganese exposure: what does it mean? Mov Disord 2002;17:568–75.

Lynam DR, Roos JW, Pfeifer GD, Fort BF, Pullin TG. Environmental effects and exposures to manganese from use of methylcyclopentadienyl manganese tricarbonyl (MMT) in gasoline. Neurotoxicology 1999;20:145–50.

Miller GW, Gainetdinov RR, Levey AI, Caron MG. Dopamine transporters and neuronal injury. Trends Pharmacol Sci 1999;20:424–9.

Mortensen OV, Amara SG. Dynamic regulation of the dopamine transporter. Eur J Pharmacol 2003;479:159–70.

Neff NH, Barrett RE, Costa E. Selective depletion of caudate nucleus dopamine and serotonin during chronic manganese dioxide administration to squirrel monkeys. Experimentia 1969;25:1140–1.

Nelson K, Golnick J, Korn T, Angle C. Manganese encephalopathy: utility of early magnetic resonance imaging. Br J Ind Med 1993;50:510–3.

Newland MC, Weiss B. Persistent effects of manganese on effortful responding and their relationship to manganese accumulation in the primate globus pallidus. Toxicol Appl Pharmacol 1992;113:87–97.

Newland MC, Ceckler TL, Kordower JH, Weiss B. Visualizing manganese in the primate basal ganglia with magnetic resonance imaging. Exp Neurol 1989;106:251–8.

Olanow CW, Good PF, Shinotoh H, Hewitt KA, Vingerhoets F, Snow BJ, et al. Manganese intoxication in the rhesus monkey: a clinical, imaging, pathologic, and biochemical study. Neurology 1996;46:492–8.

Pal PK, Samii A, Calne DB. Manganese neurotoxicity: a review of clinical features, imaging and pathology. Neurotoxicology 1999;20:227–38.

Racette BA, McGee-Minnich L, Moerlein SM, Mink JW, Videen TO, Perlmutter JS. Welding-related parkinsonism: clinical features, treatment, and pathophysiology. Neurology 2001;56:8–13.

Racette BA, Tabbal SD, Jennings D, Good L, Perlmutter JS, Evanoff B. Prevalence of parkinsonism and relationship to exposure in a large sample of Alabama welders. Neurology 2005;64:230–5.

Wong DF, Yung B, Dannals RF, Shaya EK, Ravert HT, Chen CA, et al. In vivo imaging of baboon and human dopamine transporters by positron emission tomography using [^{11}C]WIN 35,428. Synapse 1993;15:130–42.

Yamada M, Ohno S, Okayasu I, Okeda R, Hatakeyama S, Watanabe H, et al. Chronic manganese poisoning: a neuropathological study with determination of manganese distribution in the brain. Acta Neuropathol (Berl) 1986;70:273–8.